

Bifurcation structure of parameter plane for a family of unimodal piecewise smooth maps: Border-collision bifurcation curves

Iryna Sushko ^{a,*}, Anna Agliari ^b, Laura Gardini ^c

^a *Institute of Mathematics, National Academy of Sciences of Ukraine, 3 Tereshchenkivska st., 01601 Kiev, Ukraine*

^b *Faculty of Economics, Catholic University, Via Emilia Parmense 84, 29100 Piacenza, Italy*

^c *Faculty of Economics, University of Urbino, Via Saffi 42, 61029 Urbino (PU), Italy*

Abstract

We study the structure of the 2D bifurcation diagram for a two-parameter family of piecewise smooth unimodal maps f with one break point. Analysing the parameters of the normal form for the border-collision bifurcation of an attracting n -cycle of the map f , we describe the possible kinds of dynamics associated with such a bifurcation. Emergence and role of border-collision bifurcation curves in the 2D bifurcation plane are studied. Particular attention is paid also to the curves of homoclinic bifurcations giving rise to the band merging of pieces of cyclic chaotic intervals.

© 2005 Elsevier Ltd. All rights reserved.

1. Introduction

The interest towards piecewise smooth dynamical systems has been recently increased due to numerous applications in engineering, radiophysics, economics, and other sciences (see, for example, [16] and references therein). It is known that for *piecewise smooth* dynamical systems we can in general distinguish between two types of bifurcations: One includes the bifurcations which occur in *smooth* dynamical systems (either local, related to the eigenvalues crossing the unit circle, or global, such as, for example, homoclinic bifurcations), while the other is the so-called *border-collision bifurcation* [13]. This bifurcation occurs when a trajectory collides with one of the boundaries separating regions in which the function changes its definition. In general, crossing such a boundary, there is a discontinuous change in the derivative, and this may cause an abrupt transition in the structure and stability of attracting and repelling invariant sets. As a result, we may have a transition from an attracting cycle to another attracting cycle of any period, or to a cyclical chaotic attractor of any period.

The study of the bifurcations associated with piecewise smooth systems started with the works by Feigen (in the decade 1970–1980), whose results were expounded and reworked in [3], with new proofs. In that paper some analytical conditions are given related to possible consequences of a border-collision bifurcation in n -dimensional piecewise

* Corresponding author. Tel.: +38 44 234 6322; fax: +38 44 235 2010.
E-mail address: sushko@imath.kiev.ua (I. Sushko).

smooth systems. In that literature the bifurcations associated with the border points are called *C-bifurcations* (see also [4]). While the term *border-collision bifurcation* was introduced by Nusse and Yorke [13,14]. In these papers the authors examine bifurcation phenomena for 1D and 2D piecewise smooth maps and state explicitly which border-collision bifurcation does occur depending on the parameters. Their approach allows to classify border-collision bifurcations according to the right and left side derivatives of the map evaluated at border-crossing fixed point for the bifurcation parameter value. In [1] it is proposed to study the border-collision phenomena by means of a so-called *normal form*, which is the piecewise linear approximation of the map in the neighborhood of the border point. In that paper the authors give a classification of the border-collision bifurcations depending on two parameters of such a normal form, which are indeed the right and left side partial derivatives mentioned above.

Given that the normal form is a *piecewise linear map*, it becomes very useful the analysis of the bifurcation sequences allowed in such maps, performed in [8] for a unimodal piecewise linear map with one break point, that is, for so-called *skew-tent maps*. In that paper analytical expressions for all the bifurcation curves are derived, and, in particular, it is shown that for piecewise linear maps one of the most relevant characteristics is the absence of cascade of period-doubling bifurcations of periodic orbits, which are instead organized in a *period-adding* sequence. The transitions are reduced to a few cascades of band merging bifurcations of cyclical chaotic intervals caused by the homoclinic bifurcations of the relevant cycles. Similar kind of analysis for a bimodal piecewise linear map with two break points is performed in [9].

Following the economic model proposed in [2], we study the dynamic properties of a two-parameter family of piecewise smooth unimodal maps with one break point, namely, we consider the map f defined as

$$f : x \mapsto f(x) = \begin{cases} f_1(x) = rx, & \text{for } 0 \leq x < \bar{x}; \\ f_2(x) = ax(1-x), & \text{for } \bar{x} \leq x \leq 1; \end{cases} \quad \bar{x} = 1 - \frac{r}{a}, \quad (1)$$

where a and r are real parameters: $a > 3$ and $1 < r < a$.

Examples of 1D unimodal piecewise smooth maps, described in the literature, belong mainly to the class of piecewise monotone maps with an extremum in the break point (see, for example, [6,12,14]). While the map (1) allows two possibilities: (1) For $a < 2r$ the map f has a maximum at $x_c = 1/2$, $x_c > \bar{x}$; (2) For $a \geq 2r$ the map f has a maximum at the break point \bar{x} . Our purpose is to compare the bifurcation structure of the (r, a) -parameter plane in these two cases, and to investigate the emergence and role of border-collision bifurcation curves. In order to show which kinds of the border-collision bifurcations are allowed, we apply to the map f the methods and results developed in [8,14,1] (see Section 2.1). We conclude that for $a < 2r$ an attracting n -cycle of the map f can undergo either ‘period-doubling’, or ‘fold’, or ‘subcritical period-doubling’ border-collision bifurcation (we use the inverted commas in order to emphasize that these bifurcations differ from those which occur for smooth maps). While the case $a > 2r$ is richer: Besides the ‘fold’ and ‘period-doubling’, it is possible to have a border-collision bifurcation from an attracting n -cycle to an attracting kn -cycle, $k = 3, \dots, l$, where $l \rightarrow \infty$ as $n \rightarrow \infty$, as well as to a cyclic chaotic interval of period $2kn$, kn , or n , for $n \geq 3$, or to a cyclic chaotic interval of period $2^i n$, $i = 0, 1, \dots$, for $n = 2$.

The peculiarity of the case $a < 2r$ is the existence of infinitely many regions of bistability in the (r, a) -parameter plane, which are bounded by fold, period-doubling and border-collision bifurcation curves. This phenomenon has been already described in [15], and we recall briefly these results in Section 2.2. While Section 2.3 is devoted to the bifurcation structure of the (r, a) -parameter plane in case $a > 2r$. The main difference of this case is the predominance of parameter values corresponding to chaotic attractors, which become open 2D subsets, bounded by border-collision and homoclinic bifurcation curves, while for $a < 2r$ such parameter values form only 1D subsets (curves of zero measure).

2. Bifurcation structure of the parameter plane

Let us first derive some simple propositions for the map f defined in (1). In the considerations given below we assume $(r, a) \in R = \{(r, a) : a > 3, 1 < r < a\}$.

It is easy to show that the point of the local extremum (maximum) of the function (1) is the break point \bar{x} for $a \geq 2r$, and the critical point $x_c = 1/2$ for $a < 2r$. Using this property we get the condition for the interval $I = [0, 1]$ to be trapping for the map f (i.e., $f(I) \subseteq I$):

Proposition 1. *If $(r, a) \in D \subset R$, where*

$$D = \{(r, a) : r < 2, a \leq r^2/(r-1)\} \cup \{(r, a) : r \geq 2, a \leq 4\},$$

then the interval I is trapping for f .

In the (r, a) -parameter plane the curves $a = r^2/(r - 1)$ (for $r < 2$) and $a = 4$ (for $r \geq 2$), at which the interval I is invariant (i.e., $f(I) = I$), correspond to the so-called *boundary crisis* bifurcation (homoclinic bifurcation of the origin). If the (r, a) -parameter point is taken above these curves then almost all the trajectories of the map f go to infinity and the surviving set is an invariant Cantor set $A \subset I$ called a *chaotic repeller*.

We investigate the parameter range in which the interval I is trapping, i.e., we take the parameter values $(r, a) \in D$ and, thus, $f: [0, 1] \rightarrow [0, 1]$.

Regarding the map f given in (1) the results known for the logistic map are applied (for some fixed r) if the absorbing interval J of the map f is included in the interval where this map is defined by the logistic function only, i.e., if $J \subseteq [\bar{x}, 1]$, that is if $f^2(x_c) \geq \bar{x}$. The last inequality is satisfied under the condition stated in the following:

Proposition 2. *If*

$$r \geq r_1(a) \stackrel{\text{def}}{=} a^4/16 - a^3/4 + a, \tag{2}$$

then the absorbing interval $J = [f^2(x_c), f(x_c)]$ of the map (1) is included in $[\bar{x}, 1]$.

Thus, a parameter region $D_l \subset D$, for which (2) is satisfied, has the “logistic” bifurcation structure (see Fig. 1) in the following sense: In order to comment a 1D bifurcation diagram, if we fix a parameter point $(r, a) = (r^*, a^*) \in D_l$ and move it increasing a , up to the point $(r^*, a^{**}) \in r_l(a)$, then we get the 1D bifurcation diagram of the logistic map for $a \in [a^*, a^{**}]$.

Answer to the question of how many attracting cycles of the same period n exist, can be get from the theory of symbolic dynamics (see [10,5]), or from the description of the “box-within-a-box” bifurcation structure (see [11]). Now we recall only that the logistic map has k attracting cycles of the same period n for different values of a , where the corresponding values of the pair (k, n) are (1, 2), (1, 3), (2, 4), (3, 5), (5, 6), (9, 7), (16, 8), ... These k different attracting n -cycles are ordered on a according to the order of their symbolic sequences.

Let P_n denote a region in the (r, a) -parameter plane such that for $(r, a) \in P_n$ the map (1) has an attracting cycle of period n (note that we use the same notation P_n for different regions of the same periodicity, that is, there exist k different regions P_n). Fig. 1 presents a 2D bifurcation diagram of the map f in the (r, a) -parameter plane, where the regions P_n are shown by different gray tonalities for different n , $n \leq 24$. Obviously, the lower boundary of a periodicity region $P_n \cap D_l$ corresponds either to a *fold bifurcation* (giving rise to a new periodicity “box”), or to a *period-doubling bifurcation*, while its upper boundary is a period-doubling bifurcation curve.

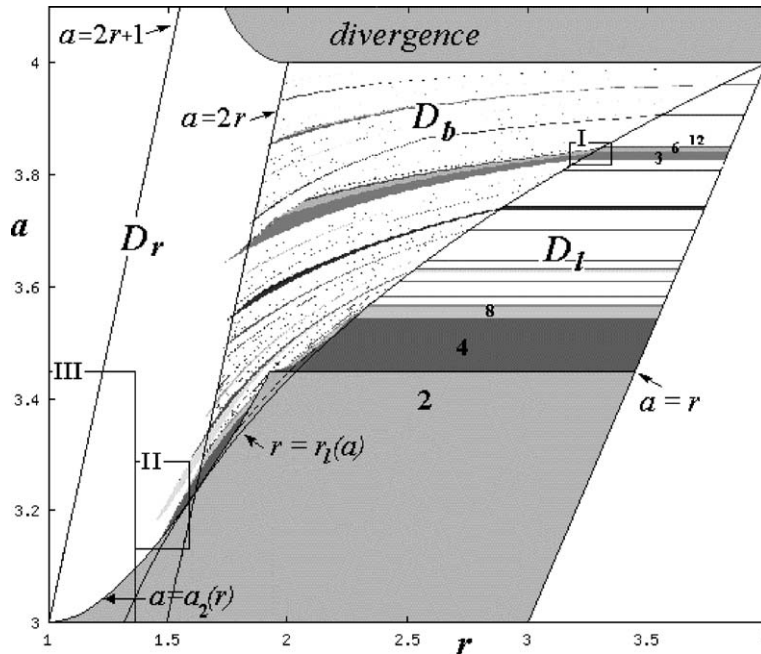


Fig. 1. 2D bifurcation diagram of the map f in the (r, a) -parameter plane. The regions P_n corresponding to attracting cycles of period n , $n \leq 24$, are shown by different gray tonalities for different n .

Let $D_b \subset D$ denote an (r, a) -parameter region defined as

$$D_b = \{(r, a) : a/2 \leq r \leq r_1(a)\},$$

where $r_1(a)$ is given in (2). For $(r, a) \in D_b$ we have $x_c \geq \bar{x}$ and $\bar{x} \in J$ (i.e., both the functions f_1 and f_2 are involved in the absorbing interval). And let $D_r \subset D$ be a region (see Fig. 1) defined as

$$D_r = \{(r, a) : a > 2r\},$$

so that for $(r, a) \in D_r$ we have $x_c < \bar{x}$, and the point of the extremum of f is the break point \bar{x} .

Our purpose is to describe the bifurcation structure of the regions D_b and D_r in order to show the emergence and role of the *border-collision bifurcation curves* which form, together with the fold and period-doubling bifurcation curves, the boundaries of the periodicity regions. To proceed we describe in the next section the different kinds of border-collision bifurcations which an attracting n -cycle of the map f can undergo.

2.1. Border-collision bifurcation of an attracting n -cycle

Let γ_{ij} denote an attracting cycle of period $n = i + j$, $i \geq 0, j > 0$, of the map f , such that i points of the cycle belong to the segment $[0, \bar{x}]$ and j points belong to $[\bar{x}, 1]$. A repelling n -cycle is denoted γ'_{ij} and a superstable n -cycle (i.e., such that x_c is a point of the cycle and, thus, its eigenvalue equals 0) is denoted $\tilde{\gamma}_{ij}$. If the numbers i and j are not specified we write γ_n, γ'_n and $\tilde{\gamma}_n$, respectively. Let G_n denote a cyclic chaotic interval of period n .

If a point of the n -cycle of the map f collides with the break point under the change in the parameters, we say that a *border-collision* (BC henceforth) occurs for this cycle. It is generally accompanied with discontinuous change in the derivative of $f(x)$ at this point. Moreover, if after such a collision the *orbit index* [14] of the border-crossing cycle changes, i.e., there is a qualitative change in the dynamics of the map, we say that a *border-collision bifurcation* (BCB henceforth) occurs for the cycle. Recall that a cycle has the orbit index 1 if its eigenvalue λ is $|\lambda| < 1, -1$ if $\lambda > 1$ and 0 if $\lambda = -1$.

Note that for $(r, a) \in P_n \cap D_r$ all the points of the corresponding attracting cycle γ_n are on the right of \bar{x} , that is we have the attracting cycle $\gamma_{0,n}$ of the logistic map f_2 . Decreasing r the distance between \bar{x} and the leftmost periodic point is decreasing so that at some value of r we have the first BC for the cycle $\gamma_{0,n}$. If after such a collision the cycle remains attracting, that is the map f has the attracting cycle $\gamma_{1,n-1}$, we can vary the (r, a) -parameter values in such a way that one more point of the cycle collides with \bar{x} approaching it from the right.

Suppose a BC occurs for the point x_1 of the attracting cycle $\gamma_n = \{x_1, \dots, x_n\}$. In other words, let x_1 be a *border-crossing fixed point* of the corresponding map $f^n: f^n(x_1) = x_1$. To specify the related parameter variation let \mathcal{B}_n denote a curve in the (r, a) -parameter plane given by

$$\mathcal{B}_n = \{(r, a) : f^n(\bar{x}) = \bar{x}\},$$

corresponding to the BC of x_1 .

BC Assumption. Let the (r, a) -parameter point cross \mathcal{B}_n transversely at some point $(r^*, a^*) \in \mathcal{B}_n$ in such a way that γ_n is attracting before the collision. Suppose also that the BC occurs only for one point of the cycle.

To see which kind of BCB can occur for γ_n , we apply to the map f^n the Theorem 3 stated in [14]: The result of the BC depends on the left and right side derivatives of f^n at $x = \bar{x}$ and $(r, a) = (r^*, a^*)$, denoted α and β , respectively:

$$\alpha = \lim_{x \rightarrow \bar{x}^-} \frac{d}{dx} f^n(x); \tag{3}$$

$$\beta = \lim_{x \rightarrow \bar{x}^+} \frac{d}{dx} f^n(x). \tag{4}$$

Moreover, we can write the normal form (see [1])

$$g(x, \varepsilon) = \begin{cases} \alpha x + \varepsilon, & x \leq 0, \\ \beta x + \varepsilon, & x \geq 0, \end{cases} \tag{5}$$

where ε is a bifurcation parameter such that as ε varies through 0, the local bifurcations of the piecewise linear map g and the piecewise smooth map f^n are of the same kind, that is, the BC occurring for the cycle γ_n of the map f at $(r, a) = (r^*, a^*) \in \mathcal{B}_n$, is of the same kind as the BC of the fixed point of the map g occurring at $\varepsilon = 0$.

The dynamics of the piecewise linear map g , called *skew-tent map*, is well studied (see [8,14,1]). It is defined by the slopes α and β of the linear functions. All possible kinds of BC of the fixed point are classified according to the partition of the (α, β) -parameter plane into subregions with qualitatively the same dynamics. These results are summarized in

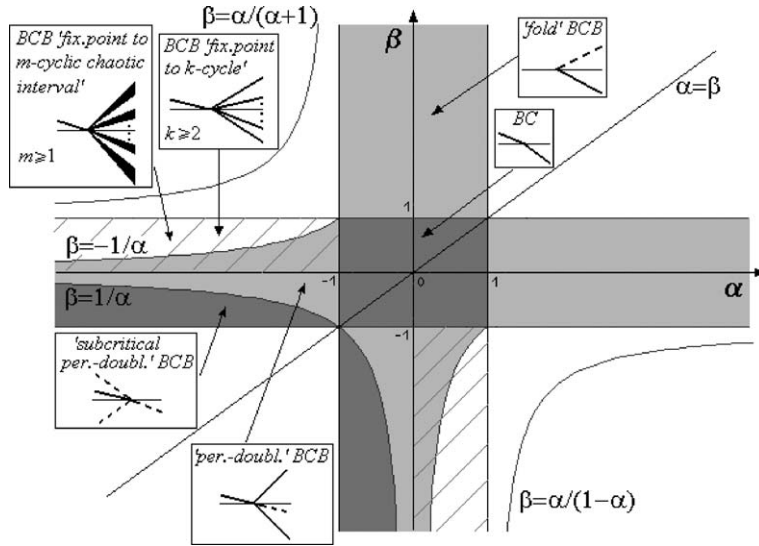


Fig. 2. The partition of the (α, β) -parameter plane into the regions with qualitatively the same dynamics of the map g at $\varepsilon < 0$ (for $\beta > \alpha$) and at $\varepsilon > 0$ (for $\beta < \alpha$). Corresponding BCB of the fixed point of g , occurring at $\varepsilon = 0$ as ε varies from $\varepsilon > 0$ to $\varepsilon < 0$, are shown schematically (the same kind of BCB occur for $\beta < \alpha$ as ε varies from $\varepsilon < 0$ to $\varepsilon > 0$): The thick and dashed lines indicate attracting and repelling cycles, respectively; the thin lines correspond to the border point.

Fig. 2. It has been studied in detail the case $0 < \alpha < 1, \beta < -1$, as well as $\alpha < -1, 0 < \beta < 1$ (see the dashed regions in Fig. 2), which are qualitatively the same cases due to the symmetry of the (α, β) -parameter plane with respect to $\alpha = \beta$. It has been shown that for $\varepsilon > 0$ ($\varepsilon < 0$, respectively), all trajectories are bounded and the map g can have an attracting cycle q_k of any period $k \geq 2$, as well as a cyclic chaotic interval Q_m of any period $m \geq 1$. It means that varying ε through 0 from $\varepsilon < 0$ to $\varepsilon > 0$ (from $\varepsilon > 0$ to $\varepsilon < 0$, respectively) we can have the BCB from the attracting fixed point to any one of such attractors. The region $\alpha > 1, \alpha/(1 - \alpha) < \beta < -1$ (and $\alpha < -1, 1 < \beta < \alpha/(\alpha + 1)$) includes subregions corresponding to the transition from no attractor to a cyclic chaotic interval Q_m of period $m = 2^k, k = 0, \dots, l$, where $l \rightarrow \infty$ as $(\alpha, \beta) \rightarrow (1, -1)$ ($(\alpha, \beta) \rightarrow (-1, 1)$, respectively).

Using the above approach we can classify the possible kinds of BCB which an attracting cycle γ_n of the map f can undergo for $(r, a) \in D_b$:

Proposition 3. Let in the BC Assumption $(r, a) = (r^*, a^*) \in \mathcal{B}_n \subset D_b$. Then depending on the parameters there can be one of the four results of the collision: (1) The bifurcation does not occur and the cycle γ_n remains attracting (BC); (2) The reverse ‘fold’ BCB; (3) The ‘period-doubling’ BCB; (4) The ‘subcritical period-doubling’ BCB.

First note that at $(r, a) = (r^*, a^*)$ we have $\gamma_n = \{\bar{x}, f(\bar{x}), f^2(\bar{x}), \dots, f^{n-1}(\bar{x})\}$. To prove the proposition we have to estimate the corresponding parameters α and β (see (3) and (4)) of the map f^n related to the cycle γ_n at $(r, a) = (r^*, a^*)$:

$$\alpha = f'_1(\bar{x})\Pi = r^*\Pi;$$

$$\beta = f'_2(\bar{x})\Pi = (2r^* - a^*)\Pi,$$

where

$$\Pi = \prod_{i=1}^{n-1} f'(f^i(\bar{x})).$$

The cycle γ_n is supposed to be attracting before the collision, thus, $|\beta| < 1$. For $(r, a) = (r^*, a^*) \in D_b$ we have $(2r^* - a^*) > 0$. Thus, depending on the sign of Π there are two cases (see Fig. 2):

- (1) If $\Pi > 0$ then $\alpha > 0, 0 < \beta < 1$, which corresponds either to the BC (for $\alpha < 1$) or to the reverse ‘fold’ BCB (for $\alpha > 1$);
- (2) If $\Pi < 0$ then $\alpha < 0, -1 < \beta < 0$, which corresponds either to the BC (for $\alpha > -1$), or to the ‘period-doubling’ BCB (for $\alpha < -1, \beta > 1/\alpha$), or to the ‘subcritical period-doubling’ BCB (for $\beta < 1/\alpha$).

In a similar way it can be shown that for $(r, a) \in D_r$ we have the possibilities indicated in Fig. 2 for $\alpha > 0, -1 < \beta < 0$ and $\alpha < 0, 0 < \beta < 1$. The last case gives great variety of possible BCB, namely, it includes the (α, β) -parameter regions corresponding to the BCB $\gamma_n \Rightarrow \gamma_{kn}$ for any $k \geq 2$, as well as $\gamma_n \Rightarrow G_{mn}$ for any $m \geq 1$.

As an example, let us state precisely which kinds of BCB the attracting cycle $\gamma_{0,2}$ of the map f can undergo. From the equality $f_2(f_1(\bar{x})) = \bar{x}$ we obtain the BCB curve \mathcal{B}_2 :

$$\mathcal{B}_2 = \left\{ (r, a) : a = a_2(r) \stackrel{\text{def}}{=} \frac{1+r+r^2}{r}, \quad 1 < r \leq r_0 \right\},$$

where $r_0 = (\sqrt{6} + \sqrt{2})/2$ is the r -coordinate of the point $d_0(r_0, a_2(r_0))$ which is the intersection point of \mathcal{B}_2 and the period-doubling bifurcation curve $a = 1 + \sqrt{6}$ (see Figs. 1 and 5). At $(r, a) \in \mathcal{B}_2$ we have $\gamma_{0,2} = \{\bar{x}, r\bar{x}\}$, $\bar{x} = (1+r)/(1+r+r^2)$. The parameters α and β of the corresponding normal form g are

$$\alpha = f'_1(\bar{x})f'_2(r\bar{x}) = 1 - r - r^2 < -1;$$

$$\beta = f'_2(\bar{x})f'_2(r\bar{x}) = (1 - r - r^2)(r^2 - r - 1)/r^2 \geq -1;$$

so that the expression for the curve \mathcal{B}_2 in the (α, β) -parameter plane is

$$\mathcal{L}_2 = \left\{ (\alpha, \beta) : \beta = \beta_2(\alpha) \stackrel{\text{def}}{=} -4\alpha \frac{\sqrt{5-4\alpha} + \alpha - 1}{(\sqrt{5-4\alpha} - 1)^2}, \quad -1 \leq \beta < 1 \right\}.$$

Now it can be seen which regions of the (α, β) -parameter plane the curve \mathcal{L}_2 crosses, and we can conclude about the BCB of the cycle $\gamma_{0,2}$: See Fig. 3 in which the corresponding bifurcation curves of the map g at $\varepsilon < 0$ are plotted using their analytical expressions derived in [8]. One has to pay attention that the considered map g is the normal form for the map f^2 , so, if the fixed point of the map g has BCB to an attractor of period n , then for the map f it corresponds to the BCB of the cycle $\gamma_{0,2}$ to an attractor of period $2n$.

Let $p_i(\alpha_i, \beta_2(\alpha_i)), i = 1, \dots$, be the intersection points of the curve \mathcal{L}_2 and the bifurcation curves of the map g in the (α, β) -parameter plane (see Fig. 3), and let $d_i(r_i, a_2(r_i))$ be the corresponding points of \mathcal{B}_2 in the (r, a) -parameter plane (the points $d_i, i = 0, 1, \dots, 8$, are indicated in Figs. 5, 9, 11). Then, based on the analytical expressions of the bifurcation curves for the map g (see [8]), we can state

Proposition 4. *The following BCB occurs for the attracting cycle $\gamma_{0,2}$ of the map f at $a = a_2(r), r \in (1, r_0)$:*

$$\{\gamma_{0,2}, \gamma'_{1,3}\} \Rightarrow \gamma'_{1,1} \text{ (the 'subcritical period-doubling' BCB) for } r \in (r_1, r_0);$$

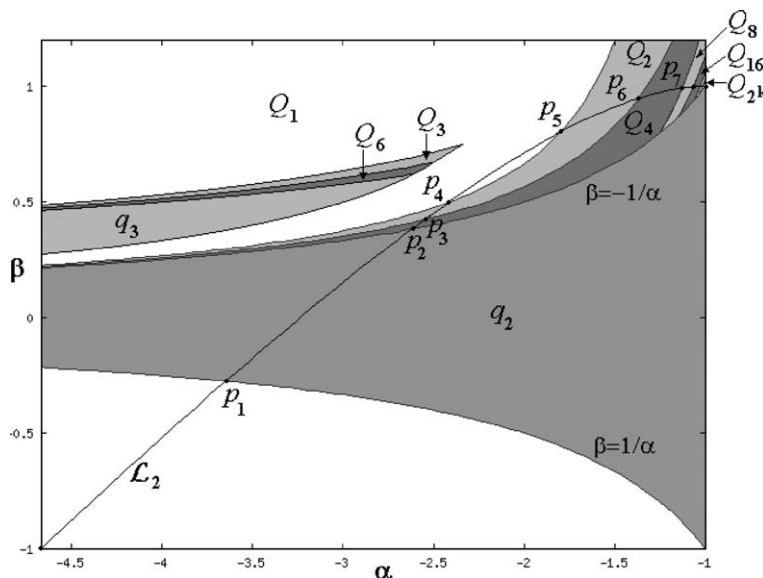


Fig. 3. A part of the (α, β) -parameter plane of the map g at $\varepsilon < 0$, where q_k denotes the region of attracting cycle of period $k = 2, 3$; regions denoted Q_m correspond to the m -cyclic chaotic intervals; the curve \mathcal{L}_2 is related to the BCB of the cycle $\gamma_{0,2}$ of the map f .

$$\begin{aligned} \gamma_{0,2} &\Rightarrow \{\gamma_{1,3}, \gamma'_{1,1}\} \text{ (the 'period-doubling' BCB) for } r \in (r_2, r_1); \\ \gamma_{0,2} &\Rightarrow G_2 \text{ for } r \in (r_5, r_4); \\ \gamma_{0,2} &\Rightarrow G_{2^2} \text{ for } r \in (r_4, r_3) \cup (r_6, r_5); \\ \gamma_{0,2} &\Rightarrow G_{2^3} \text{ for } r \in (r_3, r_2) \cup (r_7, r_6); \\ \gamma_{0,2} &\Rightarrow G_{2^{k-4}} \text{ for } r \in (r_k, r_{k-1}), k \geq 8, \text{ where } k \rightarrow \infty \text{ as } r \rightarrow 1. \end{aligned}$$

Here we write $\{\gamma_n, \gamma'_m\}$ to indicate that both cycles γ_n and γ'_m are involved in the BCB. In general, there can be infinitely many repelling cycles bifurcating from the fixed point, like, for example, when the fixed point bifurcates to a cyclic chaotic interval.

In a similar way the BCB of other attracting cycles of the map f can be investigated. As one more example, consider the attracting cycle $\gamma_{n-2,2}$ (the existence of such an attracting cycle for the map f is shown in Section 2.2). From the equality $f_1^{n-2}(f_2^2(\bar{x})) = \bar{x}$ we obtain the BCB curve

$$\mathcal{B}_n = \left\{ (r, a) : a = a_n(r) \stackrel{\text{def}}{=} \frac{1 - r^{n+1}}{(1 - r)r^{n-1}}, \quad r^* < r < r^{**} \right\},$$

where r^* and r^{**} are r -coordinates of the intersection points of \mathcal{B}_n with the curves corresponding to the fold and period-doubling bifurcations of $\gamma_{n-2,2}$, respectively. The corresponding curve \mathcal{L}_n is given by

$$\mathcal{L}_n : \begin{cases} \alpha = (1 - 2r + r^{n+1}) / (1 - r); \\ \beta = \alpha(2r^n - r^{n+1} - 1) / r^{n-2}(1 - r); \end{cases} \tag{6}$$

where $\alpha < -1$ and $-1 < \beta < 1$. It can be shown that if the (r, a) -parameter point crosses \mathcal{B}_n transversely, $\gamma_{n-2,2}$ undergoes either the 'subcritical period-doubling' BCB to $\gamma'_{n-1,1}$, or the BCB to an attracting cycle $\gamma_{n,k}$, $k = 2, \dots, l$, where $l \rightarrow \infty$ as $n \rightarrow \infty$, or to a cyclic chaotic interval $G_{n,m}$, $m = 2k, k, 1$.

As an example, see Fig. 4 in which the curve \mathcal{L}_3 given by

$$\mathcal{L}_3 : \begin{cases} \alpha = f'_1(\bar{x})f'_2(r\bar{x})f'_1(f_2(r\bar{x})) = 1 - r - r^2 - r^3; \\ \beta = f'_2(\bar{x})f'_2(r\bar{x})f'_1(f_2(r\bar{x})) = \alpha(1 - (1 + r + r^2)/r^3); \end{cases} \tag{7}$$

represents the BCB curve \mathcal{B}_3 of the attracting cycle $\gamma_{1,2}$. It can be seen that $\gamma_{1,2}$ can bifurcate to $\gamma_{3,k}$, $k = 2, 3, 4$, or to $G_{3,m}$, $m = 2k, k, 1$. Note that the only arc of \mathcal{L}_3 for $-1 < \beta < 1$ is related to the BCB of the attracting cycle $\gamma_{1,2}$. While the arc of \mathcal{L}_3 for $1 < \beta < \alpha/(\alpha + 1)$ corresponds to the BCB from no attractor to Q_1 for the map g . For the map f it is

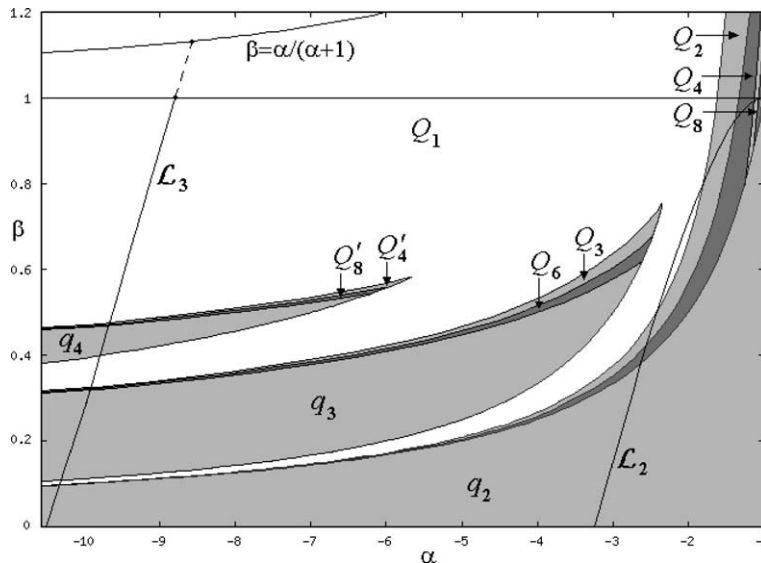


Fig. 4. A part of the (α, β) -parameter plane of the map g at $\varepsilon < 0$, where q_k denotes the region of attracting cycle of period $k = 2, 3, 4$; regions denoted Q_m and Q'_m correspond to the m -cyclic chaotic intervals; the curve \mathcal{L}_2 is related to the BCB of the cycle $\gamma_{0,2}$ of the map f and \mathcal{L}_3 to the BCB of the cycle $\gamma_{1,2}$ (the dashed arc of \mathcal{L}_3 for $1 < \beta < \alpha/(\alpha + 1)$ corresponds to the BCB to G_3).

related to the BCB which gives rise to G_3 . The curve $\beta = \alpha/(\alpha + 1)$ is related to the boundary crises for the map g , that is, for the parameter values $\beta > \alpha/(\alpha + 1)$ almost all trajectories of g go to infinity. While for the map f the arc of \mathcal{L}_3 for $\beta > \alpha/(\alpha + 1)$ has no relation to any bifurcation (the map f has a one-piece chaotic interval before and after intersection of this arc).

2.2. Bifurcation structure of the region D_b : Bistability

In this section we recall briefly some results (see [15] for the details) related to the bifurcation structure of the region D_b . Recall that for $(r, a) \in D_b$ we have $x_c \geq \bar{x}$, so the map f can have superstable cycles. The (r, a) -parameter values, corresponding to the superstable cycles of the map f form a “skeleton” of the 2D bifurcation diagram, in the same way as the values of a corresponding to the superstable n -cycles of the logistic map characterize periodic windows of the 1D bifurcation diagram. The following proposition (given in [15]) describes the border-collisions which the superstable n -cycle of the map f can undergo under specified parameter variation:

Proposition 5. *If the (r, a) -parameter point moves continuously from the right to the left inside P_n , starting from a point $(r, a) \in (P_n \cap D)$, following the corresponding superstable n -cycle of the map f , then this cycle undergoes b BC*

$$\tilde{\gamma}_{0,n} \Rightarrow \tilde{\gamma}_{1,n-1} \Rightarrow \dots \Rightarrow \tilde{\gamma}_{b,n-b},$$

after which a BCB occurs at $a = 2r$, when the critical point x_c collides with \bar{x} . Here b equals to the number of symbols L in the symbolic representation¹ of $\tilde{\gamma}_{0,n}$.

Obviously, the parameters of the normal form g given in (5) for all the BC (b in number) of $\tilde{\gamma}_n$ are $\alpha = \beta = 0$. To see that the collision of x_c with \bar{x} indeed leads to a bifurcation, we note that in this case $\beta = 0$, but α can be, in general, any real number. It can be shown (see Fig. 2) that there are three possibilities:

- (1) The ‘period-doubling’ BCB ($\alpha < -1$): The superstable n -cycle becomes unstable while an attracting $2n$ -cycle appears.
- (2) The border-collision pair bifurcation (the ‘fold’ BCB) occurring in the reverse order ($\alpha > 1$): The point x_c of the superstable n -cycle and one point of the repelling n -cycle collide with the break point and both cycles disappear.
- (3) The ‘pitchfork’ BCB occurring in the direct ($-1 < \alpha < 0$), or reverse order ($0 < \alpha < 1$). In the last case, for example, the point x_c and one more point of the superstable n -cycle, as well as one point of the repelling $n/2$ -cycle collide simultaneously with the break point and the $n/2$ -cycle becomes attracting. This BCB occurs, obviously, for the same parameter values as the ‘period-doubling’ BCB for the corresponding superstable $n/2$ -cycle.

Examples of all the three kinds of BCB of the superstable cycles of the map f can be seen in Fig. 5, which is an enlarged window of Fig. 1. The parameter paths corresponding to some superstable cycles are shown by the white curves. It can be seen that at $a = 2r$ the cycle $\tilde{\gamma}_{0,2}$ undergoes the ‘period-doubling’ BCB occurring at the same parameter values as the reverse ‘pitchfork’ BCB of the cycle $\tilde{\gamma}_{1,3}$, while the cycle $\tilde{\gamma}_{1,5}$ undergoes the reverse ‘fold’ BCB.

To illustrate Proposition 5 we present in Fig. 6 the enlarged window I of Fig. 1, with the periodicity regions P_3, P_6, P_{12}, P_{24} related to the “3-box”. Fold, period-doubling and border-collision bifurcation curves are shown by dashed, thick and thin lines, respectively. The symbolic representation of the cycle $\tilde{\gamma}_{0,3}$ is $\sum = (RLC)^\infty$, that is $b = 1$, thus, under specified parameter variation this cycle undergoes one BC $\tilde{\gamma}_{0,3} \Rightarrow \tilde{\gamma}_{1,2}$, and then the ‘period-doubling’ BCB occurs at $a = 2r$ giving rise to the cycles $\gamma_{3,3}$ and $\gamma'_{2,1}$. The symbolic representation of the considered cycle $\tilde{\gamma}_{0,6}$ is $\sum = (RL^2RLC)^\infty$, $b = 3$, thus, it undergoes three BC $\tilde{\gamma}_{0,6} \Rightarrow \tilde{\gamma}_{1,5} \Rightarrow \tilde{\gamma}_{2,4} \Rightarrow \tilde{\gamma}_{3,3}$, and then the reverse ‘pitchfork’ BCB occurs at $a = 2r$ giving rise to the attracting cycle $\gamma_{1,2}$.

Let us give one more example. It is known for the logistic map, that the symbolic representation of the last (ordered on a) superstable n -cycle is $(RL^{n-2}C)^\infty$, i.e., $b = n - 2$, thus, under the parameter variation described above, such a cycle undergoes $n - 2$ BC: $\tilde{\gamma}_{0,n} \Rightarrow \tilde{\gamma}_{1,n-1} \Rightarrow \dots \Rightarrow \tilde{\gamma}_{n-2,2}$, and then the BCB occurs when x_c collides with \bar{x} . By continuity, the map f has the attracting cycle $\gamma_{n-2,2}$ existing for the parameter values taken from some neighborhood of those corresponding to the superstable cycle $\tilde{\gamma}_{n-2,2}$. The BCB of $\tilde{\gamma}_{n-2,2}$ is described at the end of Section 2.1 from where it follows, in particular, that $\tilde{\gamma}_{n-2,2}$ undergoes the ‘period-doubling’ BCB.

¹ We refer to the symbolic representation of the superstable n -cycles $\{x_i\}_{i=1}^n$ (see [10]), which starts from the first iteration of the critical point x_c , i.e., from $x_1 = f(x_c)$. We write R if $x_i > x_c$, or L if $x_i < x_c$, or C if $x_i = x_c$, for $i = 1, \dots, n$.

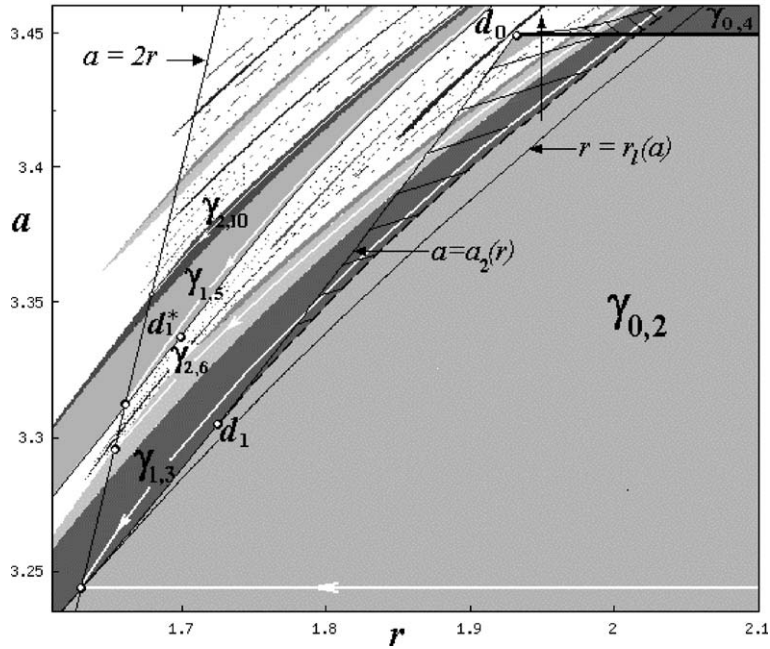


Fig. 5. An enlarged window of Fig. 1. The white curves correspond to the parameter paths of some superstable cycles; the thick straight line $a = 1 + \sqrt{6}$ is the period-doubling bifurcation curve of $\gamma_{0,2}$; the thin curves correspond to the BCB of the related cycles. The dashed regions indicate bistability.

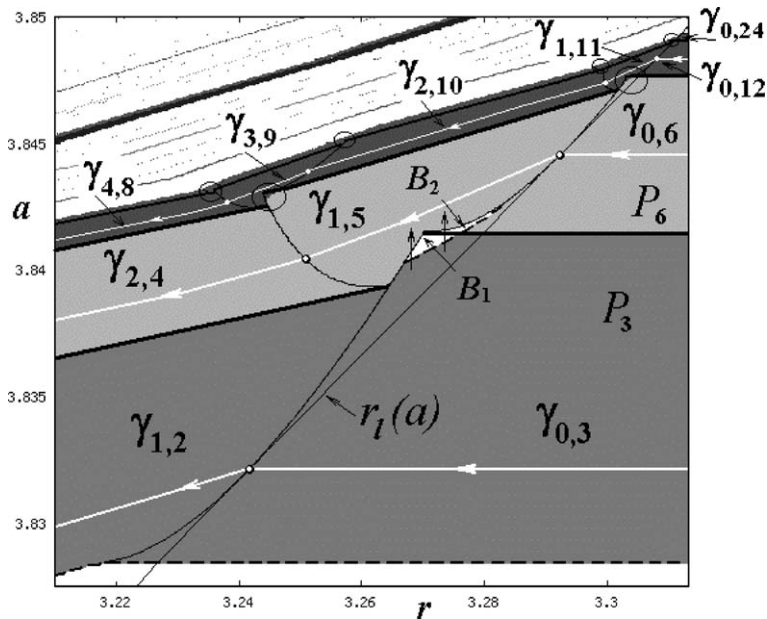


Fig. 6. The enlarged window I of Fig. 1.

It is worth to emphasize that any periodicity region P_n , with its core corresponding to the superstable n -cycles, has continuation through the whole region D_b and intersects its left boundary $a = 2r$. The boundaries of $P_n \cap D_b$ are formed by curves corresponding to fold, period-doubling and border-collision bifurcations.

Moreover, in the region D_b there are infinitely many regions of bistability corresponding to two coexisting attractors. As an example, two bistability regions B_1 and B_2 are shown in Fig. 6. To illustrate bifurcations which occur crossing different boundaries of the bistability regions, we present in Fig. 7 two 1D bifurcation diagrams (the corresponding parameter paths are indicated by the vertical straight lines with arrows in Fig. 6).

One more example of bistability is presented in Fig. 8 where one of the two branches of the 1D bifurcation diagram of the map f is shown (the corresponding parameter path is indicated in Fig. 5 by the vertical straight line with an arrow): Increasing a in the indicated range we see the attracting cycle $\gamma_{0,2}$ (thick line) coexisting at first with the attracting cycle $\gamma_{1,3}$ (thin lines) born via fold bifurcation together with the repelling cycle $\gamma'_{1,3}$ (dashed lines). Then $\gamma_{0,2}$ coexists, consequently, with all the cycles related to the period-doubling cascade of $\gamma_{1,3}$, and after with all other attractors, following the logistic bifurcation scenario (with periods multiplied by 4). One can see also that the first homoclinic bifurcation for $\gamma'_{1,3}$ results in a boundary crises for 4-cyclic chaotic intervals. Then the period-doubling bifurcation of $\gamma_{0,2}$ gives rise to an attracting cycle $\gamma_{0,4}$, and, finally, the reverse ‘fold’ BCB occurs for $\gamma_{0,4}$ and $\gamma'_{1,3}$, after which they both disappear.

2.3. Bifurcation structure of D_r : Homoclinic curves

In this section we present numerical results related to the bifurcation structure of the region D_r , main characteristic of which is the predominance of the (r, a) -parameter values corresponding to chaotic attractors with respect to the parameter values corresponding to the attracting cycles of the map f . Moreover, it is easy to check that for $a > (2r + 1)$ the map f is expanding for any point of $I = [0, 1]$, thus, in this case the map f cannot have any attracting cycle. Recall that for $(r, a) \in D_r$ we have the extremum (maximum) of f at the break point \bar{x} .

First we comment Fig. 9 which is the enlarged window II of Fig. 1. As stated in Proposition 4, if the (r, a) -parameter point crosses the BCB curve \mathcal{B}_2 , given by $a = a_2(r)$, transversely in a point between the points d_1 and d_2 (see also Fig. 5), then $\gamma_{0,2}$ bifurcates to $\gamma_{1,3}$, if it crosses between d_3 and d_2 then we have the BCB $\gamma_{0,2} \Rightarrow G_8$, if it crosses between d_4 and d_3 then the BCB $\gamma_{0,2} \Rightarrow G_4$ occurs. Increasing a the cycle $\gamma_{1,3}$ bifurcates to $\gamma_{2,6}$ due to the period-doubling bifurcation, which then undergoes the BCB to the cyclic chaotic interval G_8 (this fact can be verified by estimating the corresponding parameters α and β given in (3) and (4)).

The points d_3 and d_4 correspond to the points p_3 and p_4 in the (α, β) -plane (see Fig. 3), belonging, respectively, to the curves of the first homoclinic bifurcation of the repelling 2-cycle and the repelling fixed point of the map g . These bifurcations give rise to the pairwise merging of the pieces of the cyclic chaotic interval Q_4 (Q_2 , respectively) resulting in the chaotic interval Q_2 (Q_1). Thus, for the map f the points d_3 and d_4 , by continuity, are starting points of curves (denoted \mathcal{H}_4 and \mathcal{H}_2) corresponding to the first homoclinic bifurcation of the cycles $\gamma'_{1,3}$ and $\gamma'_{1,2}$, respectively. The curves \mathcal{H}_4 and \mathcal{H}_2 are obtained numerically. Together with the BCB curves of $\gamma_{0,2}$ and $\gamma_{2,6}$ they form the boundaries of the regions

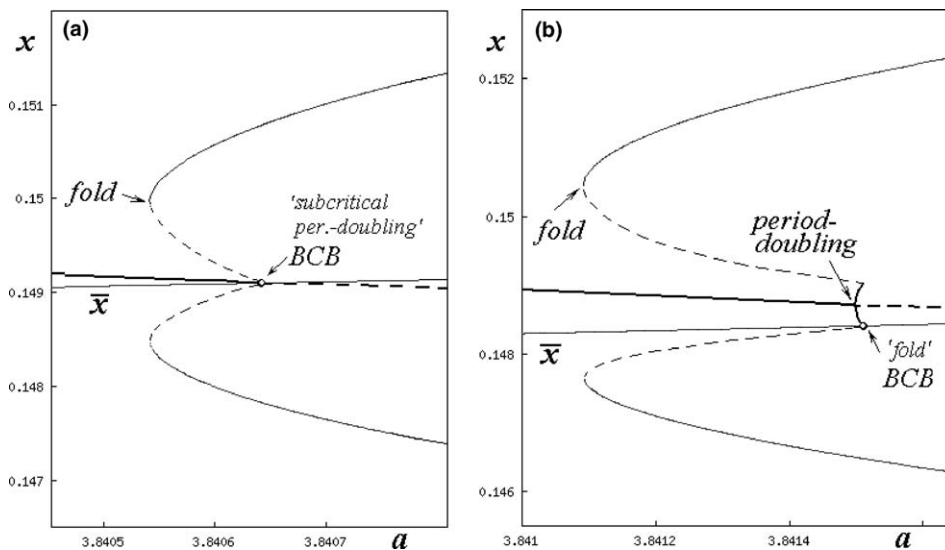


Fig. 7. One of the three branches of 1D bifurcation diagram of the map f at (a) $r = 3.268$, $a \in [3.8405, 3.8408]$ (a crossection of the bistability region B_1) and (b) $r = 3.2714$, $a \in [3.841, 3.8416]$ (a crossection of both the bistability regions B_1 and B_2).

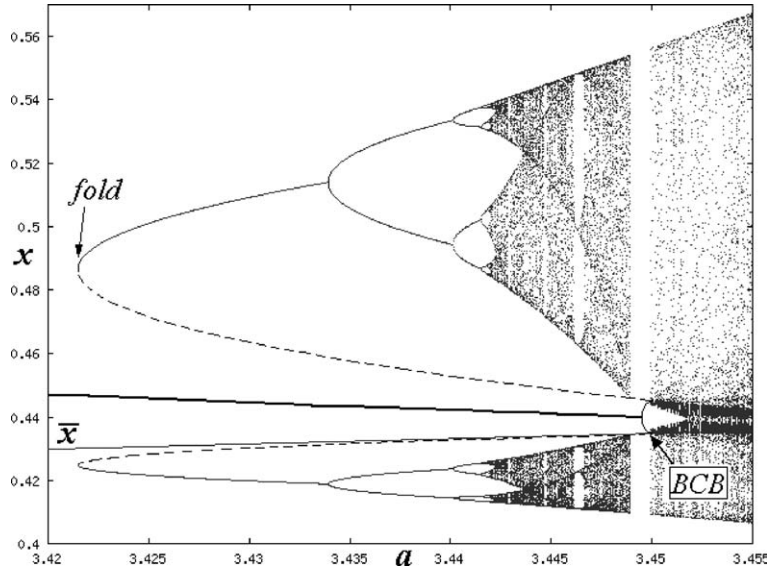


Fig. 8. One of the two branches of the 1D bifurcation diagram of the map f at $r = 1.95$, $a \in [3.42, 3.455]$.

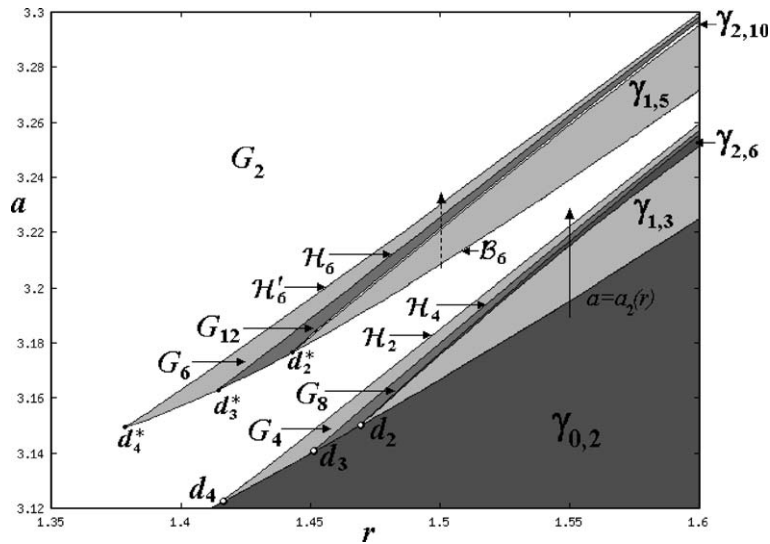


Fig. 9. The enlarged window II of Fig. 1 shows the regions corresponding to the attracting cycles $\gamma_{0,2}$, $\gamma_{1,3}$, $\gamma_{2,6}$, $\gamma_{1,5}$ and $\gamma_{2,10}$, as well as to the cyclic chaotic intervals G_8 , G_4 , G_{12} , G_6 and G_2 .

corresponding to the cyclic chaotic intervals G_8 and G_4 of the map f (for the considered parameter range). To illustrate all the bifurcations mentioned above we present in Fig. 10 one of the two branches of the 1D bifurcation diagram of the map f at $r = 1.55$, $a \in [3.19, 3.23]$ (this parameter path is indicated in Fig. 9 by the vertical straight line with an arrow).

In order to complete the consideration of the BCB of the cycle $\gamma_{0,2}$ let us comment Fig. 11 which is the enlarged window III of Fig. 1. Referring again to Proposition 4 we state that if the (r, a) -parameter point crosses transversely the BCB curve \mathcal{B}_2 in a point between d_k and d_{k-1} , $k = 5, 6, \dots$, then the BCB $\gamma_{0,2} \Rightarrow G_{2^{k-4}}$ occurs, where $k \rightarrow \infty$ as $(r, a_2(r)) \rightarrow (1, 3)$. Each the point p_k in (α, β) -parameter plane (see Fig. 3), corresponding to the point d_k , belong to the curve of the first homoclinic bifurcation of 2^{k-5} -cycle of the map g (see [8]). Thus, by continuity, the point d_k is a starting point for the curve of the first homoclinic bifurcation of the 2^{k-4} -cycle of the map f . These curves, denoted $\mathcal{H}_{2^{k-4}}$, are obtained numerically and shown in Fig. 11. If the (r, a) -parameter point crosses transversely through all the

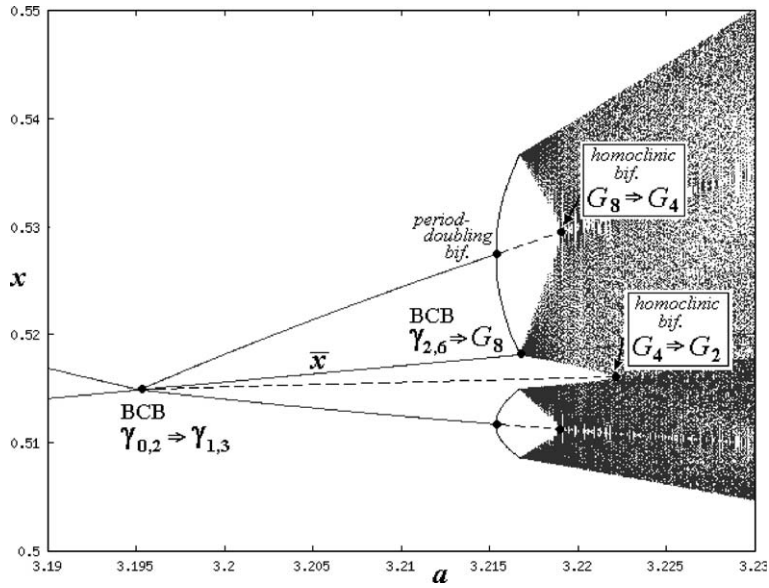


Fig. 10. One of the two branches of 1D bifurcation diagram of the map f at $r = 1.55$, $a \in [3.19, 3.23]$. Dashed lines correspond to points of the repelling cycles $\gamma'_{1,2}$ and $\gamma'_{1,3}$.

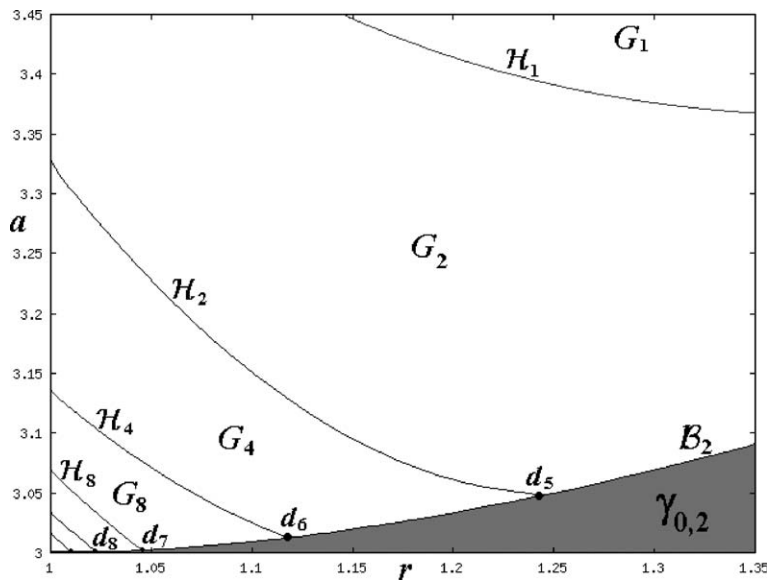


Fig. 11. The enlarged window III of Fig. 1. The curve $\mathcal{H}_{2^{k-4}}$, $k \geq 5$, corresponds to the first homoclinic bifurcation of 2^{k-4} -cycle of the map f ; the curve \mathcal{H}_1 is related to the first homoclinic bifurcation of the fixed point x^* .

curves $\mathcal{H}_{2^{k-4}}$, approaching the point $(r, a) = (1, 3)$, then we have an infinite cascade of period-doubling bifurcations for the cyclic chaotic intervals $G_2 \Rightarrow G_2^2 \Rightarrow G_2^3 \Rightarrow \dots$. The curve \mathcal{H}_1 corresponds to the first homoclinic bifurcation of the fixed point $x^* = (1 - 1/a)$ and is given by the equality $f^3(\bar{x}) = x^*$.

Now let us comment the bifurcation structure related to the region P_6 corresponding to the attracting cycle $\gamma_{1,5}$ (see Fig. 9). The lower boundary of this region, denoted \mathcal{B}_6 , corresponds to the ‘fold’ BCB giving rise to the cycles $\gamma_{1,5}$ and $\gamma_{2,4}$. Note that a ‘fold’ BCB can give rise also to two repelling cycles as we shall see below. The curve \mathcal{B}_6 is given by

$$\mathcal{B}_6 = \{(r, a) : f_2^5(f_1(\bar{x})) = \bar{x}, r_2^* < r < r_1^*\},$$

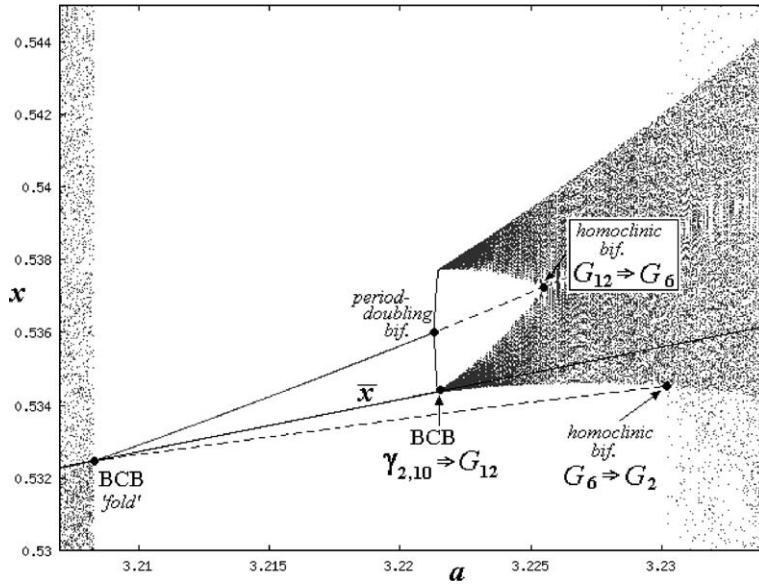


Fig. 12. One of the 6 branches of 1D bifurcation diagram for the map f at $r = 1.5$, $a \in [3.2075, 3.235]$. Dashed lines correspond to points of the repelling cycles $\gamma'_{2,4}$ and $\gamma'_{1,5}$.

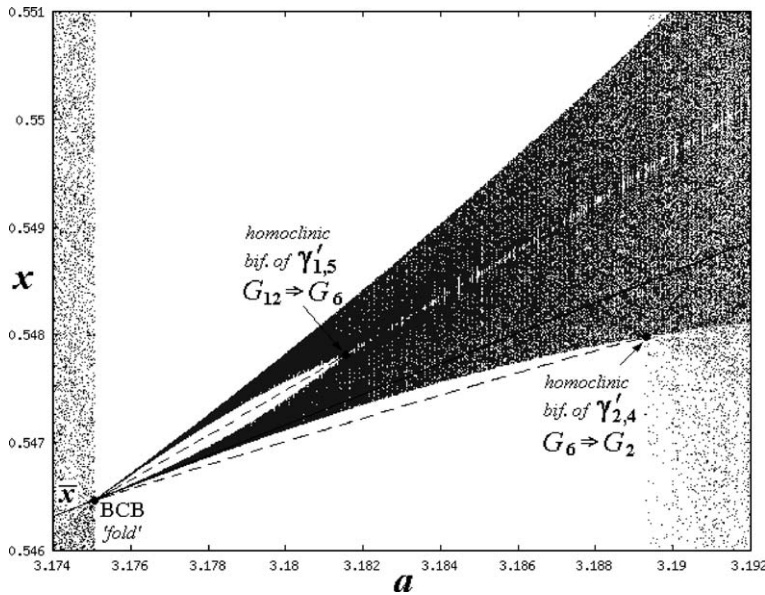


Fig. 13. One of the 6 branches of 1D bifurcation diagram of the map f at $r = 1.44$, $a \in [3.174, 3.192]$. Lower dashed line corresponds to a point of the repelling cycle $\gamma'_{2,4}$ and the upper one to a point of $\gamma'_{1,5}$, both born due to the ‘fold’ BCB, which gives rise also to the cyclic chaotic interval G_{12} .

where r_1^* is the r -coordinate of the intersection point (denoted d_1^* in Fig. 5) of \mathcal{B}_6 with the fold bifurcation curve, given by $f_2^6(x) = x$. While r_2^* is the r -coordinates of the intersection point (denoted d_2^* in Fig. 9) of \mathcal{B}_6 with the period-doubling bifurcation curve of $\gamma_{1,5}$.

Let $(r, a) \in P_6$ and a be increasing. Then the cycle $\gamma_{1,5}$ undergoes the period-doubling bifurcation giving rise to the cycle $\gamma_{2,10}$ which then undergoes the BCB to G_{12} . The first homoclinic bifurcation of the cycle $\gamma'_{1,5}$ (the related bifurcation curve is denoted \mathcal{H}_6 in Fig. 9) gives rise to the pairwise merging of the pieces of G_{12} and results in the cyclic chaotic

interval G_6 , which then bifurcate to G_2 due to the first homoclinic bifurcation of $\gamma'_{2,4}$ (the related curve is denoted \mathcal{H}'_6). As an example of such a sequence of bifurcations, Fig. 12 presents one of the 6 branches of 1D bifurcation diagram for the map f at $r = 1.5$, $a \in [3.2075, 3.235]$ (this parameter path is indicated in Fig. 9 by the vertical dashed straight line with an arrow).

We can consider also the curve \mathcal{B}_6 for $r < r_2^*$, then the arcs (d_3^*, d_2^*) and (d_4^*, d_3^*) of \mathcal{B}_6 (see Fig. 9) correspond to the ‘fold’ BCB giving rise to two repelling cycles $\gamma'_{1,5}$ and $\gamma'_{2,4}$, and to the cyclic chaotic intervals G_{12} and G_6 , respectively. Fig. 13 shows one of the 6 branches of 1D bifurcation diagram for the map f at $r = 1.44$, $a \in [3.174, 3.192]$ illustrating the ‘fold’ BCB which results in G_{12} , $\gamma'_{1,5}$ and $\gamma'_{2,4}$. To prove that such bifurcations occur one has to consider the curve \mathcal{L}_6 corresponding to \mathcal{B}_6 in the (α, β) -parameter plane (see (3) and (4)) to see which subregions this curve intersects.

3. Concluding remarks

In the present paper we have discussed the structure of the 2D bifurcation diagram of the unimodal piecewise smooth map f given in (1), both in the case in which the map f has its extremum at the break point \bar{x} , and in case in which the extremum is at a point different from \bar{x} , that is at $x_c = 1/2$. Such a difference influences the dynamics of the map: In the first case we have predominance of chaotic dynamics, with open regions in the parameter plane corresponding to chaotic trajectories, while in the second case the dynamics are mainly periodic. Comparing the possible kinds of border-collision bifurcations which an attracting n -cycle can undergo, we have seen that the first case gives rise to more possibilities, such as the BCB to an attracting kn -cycle, $k = 2, \dots, l$, where $l \rightarrow \infty$ as $n \rightarrow \infty$, as well as to a cyclic chaotic interval of period $2kn$, kn , n . While in the second case either ‘period-doubling’, or ‘fold’, or ‘subcritical period-doubling’ BCB can occur.

An interesting and open problem is to describe the border-collision bifurcation of chaotic attractors, well as to classify bifurcations of codimension two involving the border-collision bifurcations, which occur for the parameter values corresponding to the intersection of the border-collision bifurcation curves with other bifurcation curves (see [7] where a strategy for such a classification is proposed in case of piecewise smooth systems of ordinary differential equations).

Acknowledgements

The research of I. Sushko was supported by a Marie Curie International Fellowship within the 6th European Community Framework Programme. A. Agliari and L. Gardini have performed this work within the activity of the National Research Project “Nonlinear models in economic and finance: interactions, complexity and forecasting”, MIUR, Italy.

References

- [1] Banerjee S, Karthik MS, Yuan G, Yorke JA. Bifurcations in one-dimensional piecewise smooth maps—theory and applications in switching circuits. *IEEE Trans Circuits Syst I: Fund Theory Appl* 2000;47(3):389–94.
- [2] Day R. Irregular growth cycles. *Am Econom Rev* 1982;72(3):406–14.
- [3] Di Bernardo M, Feigen MI, Hogan SJ, Homer ME. Local analysis of C -bifurcations in n -dimensional piecewise smooth dynamical systems. *Chaos, Solitons & Fractals* 1999;10(11):1881–908.
- [4] Halse C, Homer M, di Bernardo M. C -bifurcations and period-adding in one-dimensional piecewise-smooth maps. *Chaos, Solitons & Fractals* 2003;18:953–76.
- [5] Hao BL. *Elementary symbolic dynamics and chaos in dissipative systems*. Singapore: World Scientific; 1989.
- [6] Ito S, Tanaka S, Nakada H. On unimodal transformations and chaos II. *Tokyo J Math* 1979;2:241–59.
- [7] Kowalczyk P, di Bernardo M, Champneys AR, Hogan SJ, Homer M, Kuznetsov YuA, et al. Two-parameter nonsmooth bifurcations of limit cycles: classification and open problems. *Int J Bifurcat Chaos*, submitted for publication.
- [8] Maistrenko YuL, Maistrenko VL, Chua LO. Cycles of chaotic intervals in a time-delayed Chua’s circuit. *Int J Bifurcat Chaos* 1993;3(6):1557–72.
- [9] Maistrenko YuL, Maistrenko VL, Vikul SI. On period-adding sequences of attracting cycles in piecewise linear maps. *Chaos, Solitons & Fractals* 1998;9(1):67–75.
- [10] Metropolis N, Stein ML, Stein PR. On finite limit sets for transformations on the unit interval. *J Comb Theory* 1973;15:25–44.
- [11] Mira C. *Chaotic dynamics*. Singapore: World Scientific; 1987.
- [12] Misiurewicz M, Kuczynski AL. Periodic orbits for interval maps with sharp cusps. *Physica D* 1991;52:191–203.
- [13] Nusse HE, Yorke JA. Border-collision bifurcations including period two to period three for piecewise smooth systems. *Physica D* 1992;57:39–57.

- [14] Nusse HE, Yorke JA. Border-collision bifurcations for piecewise smooth one-dimensional maps. *Int J Bifurcat Chaos* 1995;5(1):189–207.
- [15] Sushko I, Agliari A, Gardini L. Bistability and border-collision bifurcations for a family of unimodal piecewise smooth maps. *Discrete Contin Dynam Syst Ser B* 2005;5(3):881–97.
- [16] Zhusubaliyev ZT, Mosekilde E. *Bifurcations and chaos in piecewise-smooth dynamical systems*. Singapore: World Scientific; 2003.